Journal of Applied Mechanics and Technical Physics, Vol. 44, No. 3, pp. 395–399, 2003

CELLULAR AND TULIP FLAME CONFIGURATIONS

A. G. Istratov,[1] N. I. Kidin,[2] and A. V. Fedorov[2]

UDC 536.468

Flame propagation in a plane channel with the formation of tulip and cellular configurations of the combustion front is simulated. The near-flame flow structure and the thermal flow structure are determined. An analogy is found between the tulip configuration and flame inflections at cell interfaces.

Key words: *channel combustion, cellular and tulip flame configurations, mathematical simulation.*

At present, significant experimental and theoretical data are available on the origination and behavior of cellular and tulip flame configurations during flame propagation in a channel [1–8]. However, the hydrodynamic and thermal structures of these flames have been not clearly understood. There is some disagreement on the nature and reasons for their formation. It is of interest to compare the cellular and tulip flames.

In the present work, we consider combustion of a uniformly stirred gaseous mixture in a plane rectangular channel. One end of the channel is open and the other is closed.

Formulation of the Problem. We assume that combustion is simulated by an irreversible one-stage reaction and is described by the Arrhenius formula. The heat transfer to the walls and the influence of gravity are neglected. The viscosity ν and heat conductivity χ are assumed to be constant. We consider the case where $\chi = D = \nu$ (D is the diffusion coefficient). During laminar flame propagation, the flow is substantially subsonic; therefore, the gas is assumed to be dynamically incompressible because its density is independent of pressure drops due to hydrodynamic flows but varies with combustion temperature.

Under these assumptions, the unsteady dynamic and thermal gas parameters in the channel obey the following system of equations:

$$\frac{\partial \rho}{\partial t} + \nabla(\rho \boldsymbol{V}) = 0, \qquad \frac{\partial \rho \boldsymbol{V}}{\partial t} + (\boldsymbol{V}\cdot\nabla)\rho\boldsymbol{V} = -\nabla p + \frac{1}{\mathrm{Re}}\,\Delta \boldsymbol{V},$$

$$\frac{\partial T}{\partial t} + (\boldsymbol{V}\cdot\nabla)T = \frac{1}{\mathrm{Re}\,\mathrm{Pr}\,\rho}\,\Delta T - \frac{\mathrm{Re}\,\mathrm{Pr}\,\mathrm{Ze}^2(\varepsilon-1)\varepsilon}{2}\,a\exp\Big(\frac{E}{T_\mathrm{b}} - \frac{E}{T}\Big),$$

$$\frac{\partial a}{\partial t} + (\boldsymbol{V}\cdot\nabla)a = \frac{1}{\mathrm{Re}\,\mathrm{Pr}\,\rho}\,\Delta a - \frac{\mathrm{Re}\,\mathrm{Pr}\,\mathrm{Ze}^2\varepsilon}{2}\,a\exp\Big(\frac{E}{T_\mathrm{b}} - \frac{E}{T}\Big).$$

Here ρ is the density, p is the dynamic component of pressure, $\boldsymbol{V}$ and T are the gas velocity and temperature, T_b is the temperature of the adiabatically burnt gas, a is the concentration, E is the activation energy, t is the time, $\mathrm{Re} = u_\mathrm{n} d\rho_0/\nu$, $\mathrm{Pr} = \nu c_p/\chi = 1$, and $\mathrm{Ze} = (\varepsilon-1)E/\varepsilon^2$ are the Reynolds, Prandtl, and Zel'dovich numbers, $\varepsilon = T_\mathrm{b}/T_0$ is the coefficient of thermal expansion of the gas, d is the channel width, c_p is the heat capacity at constant pressure, and u_n is the normal laminar-flame velocity calculated by the Zel'dovich–Frank-Kamenetskii formula. The Lewis number is $\mathrm{Le} = \chi/(c_p\rho_0 D) = 1$ and the Mach number is $\mathrm{M} \ll 1$. The static pressure in the channel is assumed to be constant and equal to the atmospheric value.

The problem was solved in the region $x \in [0,4]$ and $y \in [0,1]$. Ignition was initiated by either a hot spot or a layer near the open end of the channel. In this case, we obtain $T(x,y) = T_0 + (T_\mathrm{b} - T_0)[\tanh\,(r+dr) - \tanh\,(r-dr)]/2$, where $r = x - x_0$ for the first case and $r = (x-x_0)^2 + (y-y_0)^2$ for the second case. The value of dr is of the

[1] Institute of Chemical Physics, Russian Academy of Sciences, Moscow 117977. [2] Institute of Problems of Mechanics, Russian Academy of Sciences, Moscow 117526. Translated from Prikladnaya Mekhanika i Tekhnicheskaya Fizika, Vol. 44, No. 3, pp. 112–116, May–June, 2003. Original article submitted July 24, 2002.

0021-8944/03/4403-0395 $25.00

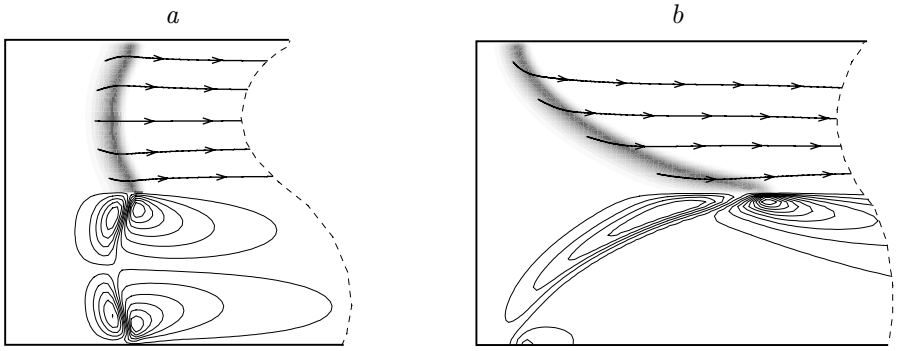

Fig. 1. Schlieren pictures of the temperature field with the streamlines of the cellular (a) and tulip (b) flame configurations (at the top) and vorticity isolines (at the bottom).

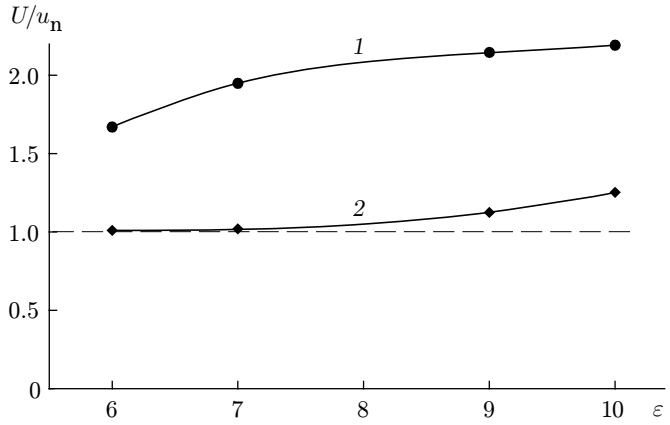

Fig. 2. Propagation velocities $U/u_{\rm n}$ of the "tulip" (1) and cellular flames as a whole (2) versus the degree of thermal expansion ε.

order of the front thickness. The density during ignition was calculated from the temperature distribution. The system was solved under both no-slip ($\boldsymbol{V} = 0$) and slip $[(\partial \boldsymbol{V}/\partial \boldsymbol{n})_w = 0]$ conditions on the wall. The boundary was considered impermeable $[(\boldsymbol{n} \cdot \nabla a)_w = 0]$ or adiabatic $[(\boldsymbol{n} \cdot \nabla T)_w = 0]$.

The calculations were performed on a uniform grid by an explicit scheme with splitting in physical processes. Poisson's equations for determining the dynamic component of pressure were solved using the ISIS++ software.

Numerical Simulation Results. Cellular flames (Fig. 1a) are formed by gas slipping on the channel walls. The streamlines are constructed by the velocity field in a fixed coordinate system. The slip conditions on the wall are similar to those on the cell interface, which allows us to increase the number of cells along the front by increasing the channel width, i.e., the number of cells increases with increasing Reynolds number (Re).

The "tulip" configuration (Fig. 1b) is formed by both the no-slip conditions on the wall and flame propagation from the open channel end. The "tulip" remains unchanged until it almost touches the wall closing the channel.

The propagation velocities of the "tulip" and cellular flames exceed those of the plane flame and depend on the degree of thermal expansion of the gas (Fig. 2).

The streamlines of the gas flow through the "tulip" and cells are identical. The "tulip" taper and the inflections of the smooth flame surface at the cell interfaces appear as hydrodynamic sinks (see Fig. 1). The flow of combustion products behind the "tulip" or cells is vortical. It is worth noting that vorticity also occurs inside the flame front and is due to the flow turning during thermal expansion. The sign of vorticity in combustion products is opposite to the sign of vorticity in the flame front.

Configurations of the cell inflections and tulip-flame edge can be converged into each other through an affine transformation (Fig. 3a). The coefficients of transformation along the x and y axes, necessary to superpose these inflections, are functions of thermal expansion. It is established that the coefficient of transformation along the x

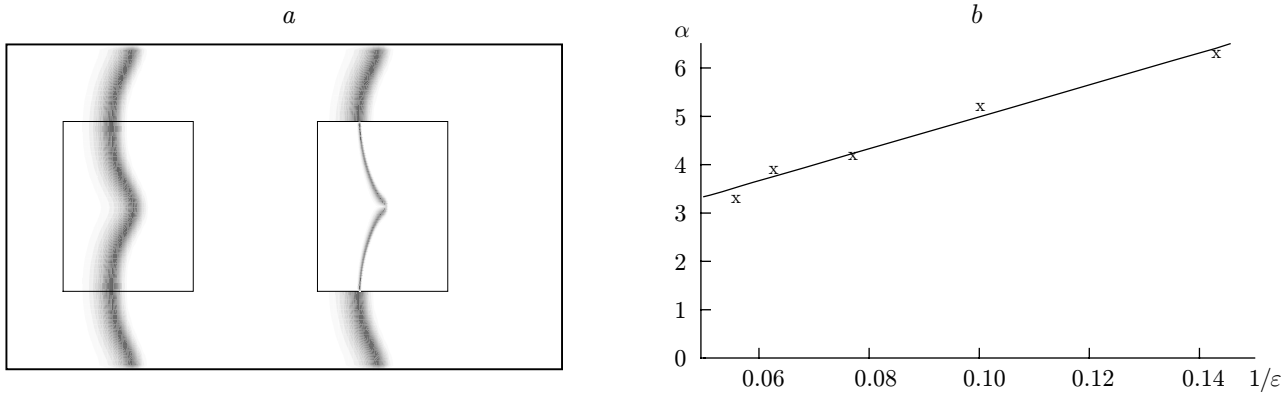

Fig. 3. Affine conversion of the "tulip" to the cellular flame (a) and the dependence of the coefficient of this conversion α on the degree of thermal expansion (b): the points show the calculated data and the curve is their approximation.

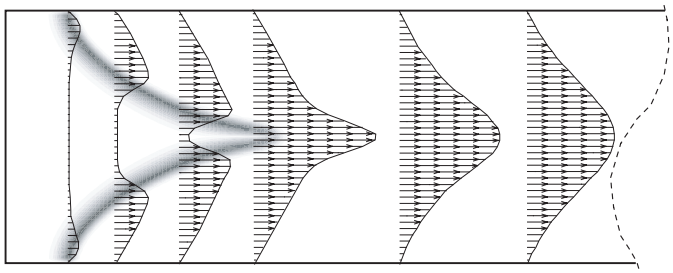

Fig. 4. Diagrams of the velocity field of the tulip flame.

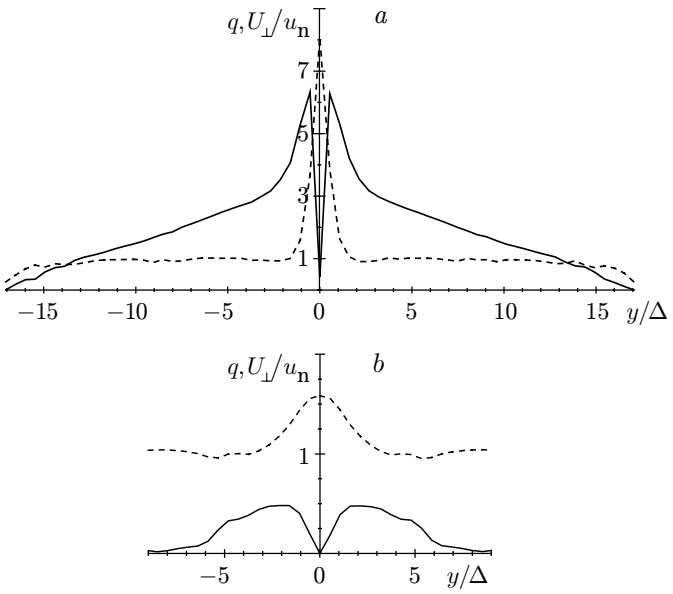

Fig. 5. Heat flux and burning rate along the front versus the distance y normalized to the flame-front thickness Δ, up to the inflections of the "tulip" (a) and the cell (b): the solid curves refer to $q = \rho U_\parallel c_p T/(\rho_0 u_\mathrm{n} c_p T_0)$ and the dashed curves refer to $U_\perp/u_\mathrm{n}$.

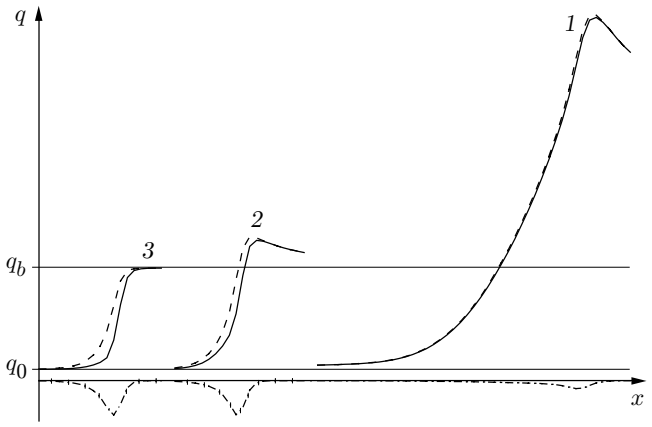

Fig. 6. Heat fluxes for the "normal" flame and along the axis passing through the flame inflection: 1) tulip configuration; 2) cellular configuration; 3) "normal" configuration; the dashed, dot-and-dashed, and solid curves refer to the convective, conductive, and total flux, respectively.

axis is inversely proportional to Re. The coefficient of transformation along the y axis is proportional to $1/\mathrm{Re}$ due to the increase in the number of cells with increasing Re. Thus, the ratio of the coefficients of transformation along the x and y axes is independent of the Reynolds number. The dependence of this ratio on the degree of thermal expansion is shown in Fig. 3b.

Figure 4 shows successive diagrams of the velocity fields of the flow induced by the "tulip" configuration. Strong inhomogeneity of the velocity field is observed in the neighborhood of the "tulip" taper, which is smoothed out afterwards.

The thermal structure of the "tulip" front is subject to the so-called stretch-effect caused by the tangential gas velocity variable along the front [9, 10]. Because of this effect, the joining of the thermal structure in the vicinity of the taper (giving rise to the region with an elevated burning rate) (Fig. 5) is similar to that observed at the flame top in the Bunsen burner. The latter is mainly due to the convective rather than conductive heat fluxes (Fig. 6). The convective heat flux in the front regions closing the "tulip" taper is much larger than the flux for the "normal" flame.

The stretch-effect on the cell inflections is substantially weaker.

Conclusions. Numerical simulation of flame propagation resulting in "tulip" and cellular flames in a plane channel for Lewis and Prandtl numbers equal to unity has revealed an analogy between the "tulip" taper and flame inflections at cell interfaces. The taper and inflections are hydrodynamic sinks for the fuel mixture. In combustion products, vorticity and substantial flow inhomogeneity are observed. The front-propagation velocity and burning rate in the "tulip" taper and cellular flame inflections are higher than in the remaining sections of the front. In these regions, the convective heat fluxes are substantial.

REFERENCES

1. G. H. Markstein, *Nonsteady Flame Propagation*, Pergamon Press, New York (1964).
2. D. Dunn-Runkin, P. K. Berr, and R. F. Sawyer, "Numerical and experimental study of 'tulip' flame formation in a closed vessel," in: *Proc. of the 21st Intern. Symp. on Combustion*, Combust. Inst., Pittsburg (1986), pp. 1291–1301.
3. S. T. Lee and C. H. Tsai, "Numerical investigation of steady laminar flame propagation in a circular tube," *Combust. Flame*, **99**, 484–490 (1994).
4. M. Gonzalez, R. Borghi, and A. Saouab, "Detailed analysis of tulip flame phenomenon using numerical simulation," *Combust. Flame*, **88**, 201–220 (1992).
5. M. Gonzalez, "Acoustic instability of a premixed flame propagation in a tube," *Combust. Flame,* **107**, 245–259 (1996).

6. C. Hackert, J. L. Ellzey, and O. A. Ezekoye, "Effect of thermal boundary conditions of flame shape and quenching in ducts," *Combust. Flame*, **112**, 73, 74 (1998).
7. V. Karlin, G. Makhviladze, J. Roberts, and V. I. Melikhov, "Effect of Lewis number of flame front fragmentation in narrow closed channels," *Combust. Flame*, **120,** 173–187 (2000).
8. Ya. B. Zel'dovich, A. G. Istratov, N. I. Kidin, and V. B. Librovich, *Flow Hydrodynamics and Curved Front Stability During Flame Propagation in Channels*, Preprint No. 143, Inst. of Problems of Mechanics, Acad. of Sci. of the USSR, Moscow (1980).
9. B. Karlovitz, D. W. Jr. Denniston, D. H. Knapschaefer, and F. E. Wells, "Studies on turbulent flames," in: *Proc. of the 4th Int. Symp. on Combustion*, Williams and Wilkins, Baltimore (1953), pp. 613–620.
10. A. M. Klimov, "Laminar flame in a turbulent flow," *Prikl. Mekh. Tekh. Fiz.*, No. 3, 49–58 (1963).